3-2015

Hydroclimatic shifts in northeast Thailand during the last two millennia — The record of Lake Pa Kho

Sakonvan Chawchai
Stockholm University, sakonvan.chawchai@geo.su.se

Akkaneewut Chabangborn
Stockholm University

Sherilyn C. Fritz
University of Nebraska-Lincoln, sfritz2@unl.edu

Minna Väliranta
University of Helsinki

Carl-Magnus Mörth
Stockholm University

See next page for additional authors

Authors

Sakonvan Chawchai, Akkaneewut Chabangborn, Sherilyn C. Fritz, Minna Väliranta, Carl-Magnus Mörth, Maarten Blaauw, Paul J. Reimer, Paul J. Kusic, Ludvig Löwemark, and Barbara Wohlfarth

Nebraska
UNIVERSITY OF
Lincoln
digitalcommons.unl.edu

Hydroclimatic shifts in northeast Thailand during the last two millennia — The record of Lake Pa Kho

Sakonvan Chawchai,[1,2] Akkaneewut Chabangborn,[1,2] Sherilyn Fritz,[3] Minna Väliranta,[4] Carl-Magnus Mörth,[1] Maarten Blaauw,[5] Paula J. Reimer,[5] Paul J. Krusic,[6] Ludvig Löwemark,[7] and Barbara Wohlfarth[1]

1. Department of Geological Sciences, Stockholm University, Stockholm 10691, Sweden
2. Department of Geology, Faculty of Science, Chulalongkorn University, Bangkok 10330, Thailand
3. Department of Earth and Atmospheric Sciences and School of Biological Sciences, University of Nebraska–Lincoln, NE 68588-0340, USA
4. Department of Environmental Sciences, University of Helsinki, Helsinki 4603, Finland
5. Centre for Climate, the Environment & Chronology (14CHRONO), School of Geography, Archaeology and Palaeoecology, Queen's University of Belfast, Belfast BT7 1NN, UK
6. Department of Physical Geography and Quaternary Geology, Stockholm University, Stockholm 10691, Sweden
7. Department of Geosciences, National Taiwan University, Taipei 106, Taiwan

Corresponding authors — S. Chawchai & B. Wohlfarth, Department of Geological Sciences, Stockholm University, Stockholm 10691, Sweden; email addresses: sakonvan.chawchai@geo.su.se & barbara.wohlfarth@geo.su.se

Abstract

The Southeast Asian mainland is located in the central path of the Asian summer monsoon, a region where paleoclimatic data are still sparse. Here we present a multi-proxy (TOC, C/N, $\delta^{13}C$, biogenic silica, and XRF elemental data) study of a 1.5 m sediment/peat sequence from Lake Pa Kho, northeast Thailand, which is supported by 20 AMS ^{14}C ages. Hydroclimatic reconstructions for Pa Kho suggest a strengthened summer monsoon between BC 170–AD 370, AD 800–960, and after AD 1450; and a weakening of the summer monsoon between AD 370–800, and AD 1300–1450. Increased run-off and a higher nutrient supply after AD 1700 can be linked to agricultural intensification and land-use changes in the region. This study fills an important gap in data coverage with respect to summer monsoon variability over Southeast Asia during the past 2000 years and enables the mean position of the Intertropical Convergence Zone (ITCZ) to be inferred based on comparisons with other regional studies. Intervals of strengthened/weaker summer monsoon rainfall suggest that the mean position of the ITCZ was located as far north as 35°N between BC 170–AD 370 and AD 800–960, whereas it likely did not reach above 17°N during the drought intervals of AD 370–800 and AD 1300–1450. The spatial pattern of rainfall variation seems to have changed after AD 1450, when the inferred moisture history for Pa Kho indicates a more southerly location of the mean position of the summer ITCZ.

Keywords: wetland/peatland, geochemistry, paleoclimate, last two millennia, Asian monsoon

1. Introduction

The Asian summer monsoon during the past 2000 years was generally weaker than in the early Holocene in response to the long-term decline in summer insolation (Y. Wang et al., 2005). Yet high-resolution tree ring (Cook et al., 2010), marine (Anderson et al., 2002; Newton et al., 2006; Oppo et al., 2009), coral (Cobb et al., 2003), speleothem (Sinha et al., 2011a; Zhang et al., 2008), and lake (Yancheva et al., 2007) studies show that substantial decadal to centennial variations in summer monsoon intensity were superimposed on the long-term trend. Various hypotheses have been brought forward

to explain this decadal to centennial-scale variability, including solar forcing (Zhang et al., 2008); El Niño Southern Oscillation (ENSO) (Cobb et al., 2003; Mann et al., 2009) and Indo-Pacific climate variability (Prasad et al., 2014; Ummenhofer et al., 2013); movement of the mean position of the Intertropical Convergence Zone (ITCZ) (Newton et al., 2006; Sachs et al., 2009; Tierney et al., 2010); and changes in the Indian Ocean Dipole (Ummenhofer et al., 2013) and Pacific Walker Circulation (Yan et al., 2011).

The most detailed reconstructions of decadal and subdecadal shifts in summer monsoon strength are derived from the network of Asian tree ring sites (MADA) extending back
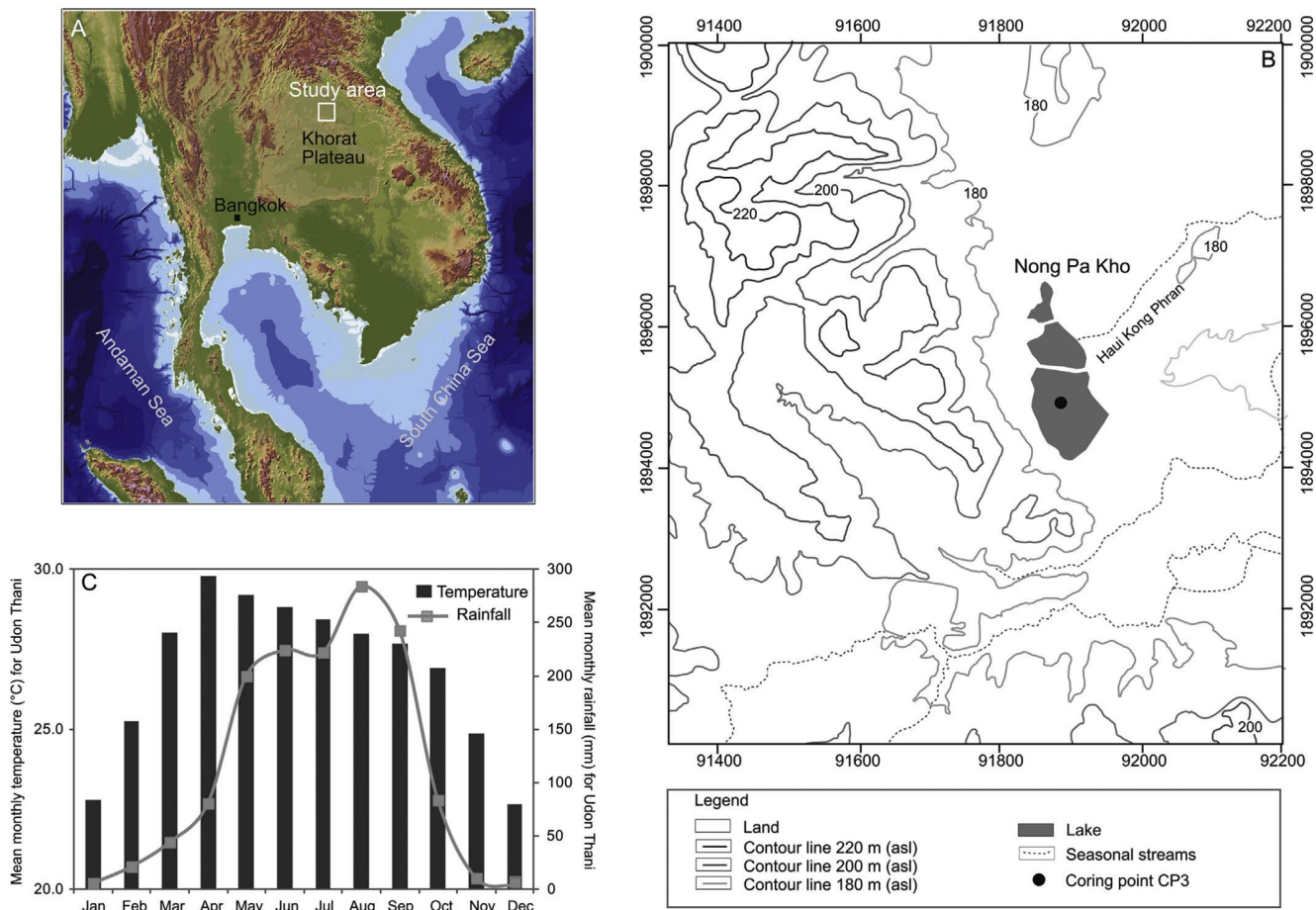
Figure 1. (A) Location of the study area in northeast Thailand. (B) Topography around Nong Pa Kho and the location of coring point CP3. The coordinate system is based on the UTM Grid system (WGS 1984 zone 48; asl = above sea level). (C) Mean monthly rainfall and temperature (1962–2011) for Udon Thani, which is situated 36 km NW of Pa Kho. Map (A) was generated using the generic mapping tools-GMT (http://gmt.soest.hawaii.edu/), and map (B) was redrawn based on aerial photographs before and after 1994 using the data set in Klubseang (2011).

through the last millennium (Cook et al., 2010; Pages 2K, Consortium, 2013). MADA and key speleothem records from China and India suggest, for example, a general weakening of the summer monsoon between AD 1400–1800 and a link between intense droughts during the 14th and 15th centuries and the demise of ancient societies in various parts of Asia (Buckley et al., 2010, 2014; Sinha et al., 2011b; Zhang et al., 2008).

The Asian monsoon system is comprised of several subsystems whose modern interactions are complex, with considerable spatial variation in monsoon intensity and frequency (Wang et al., 2005a; Wang, 2009). The Indian, the East Asian, and the Western North Pacific summer monsoon subsystems influence the Southeast Asian mainland, but how these systems interacted to affect the spatial pattern of past drought is not well resolved. Tree ring records generally span less than 1000 years and have gaps in spatial coverage, and other palaeoenvironmental data for the Southeast Asian mainland are still sparse. Thus, additional regional records are critical to fully resolve spatial patterns of Asian monsoon variation during the late Holocene, a key step in understanding long-term monsoon dynamics and potential monsoon responses to changing global climate conditions.

Here we develop a high-resolution palaeoenvironmental data series (TOC, C/N, $\delta^{13}C$, biogenic silica, and XRF elemental data) supported by 20 accelerator mass spectrometer (AMS) ^{14}C ages, from a 1.5 m long sediment/peat sequence from Lake (Nong) Pa Kho in northeast Thailand (Figure 1A). The site is

located close to the present boundary between the East Asian and Indian Ocean monsoon domains at 105°E (P. Wang et al., 2005), and is affected by the seasonal migration of the summer monsoon and of the ITCZ.

2. Regional setting

Lake Pa Kho (17° 06′ N, 102° 56′ E; 175 m above sea level; <3 km²) is presently a dammed lake that flooded a former wetland (Penny, 2001). Several dams (built between 1989 and 2004) divide the lake into three sub-basins of different size (Figure 1B). Low hills to the west and south rise to ~230 m above sea level (Figure 1B) and are the source of small seasonal streams that feed neighboring Lake Kumphawapi. The flat area surrounding the lake is primarily used as paddy fields, and for sugar cane and *Eucalyptus* plantations. The bedrock underlying the alluvial sediments is mainly composed of Cretaceous and Neogene sand and siltstones (El Tabakh et al., 2003; Wannakomol, 2005).

Climate in the region is tropical monsoonal, with mean air temperatures of ~22°–25 °C from November to February and 27°–30 °C from March to October (Figure 1C). Mean annual precipitation is ~1455 mm, 88% of which falls from May to October. Thailand's tropical/sub-tropical monsoon shows a strong correlation with indices of the Indian summer monsoon and the Western North Pacific summer monsoon during the instrumental period (Limsakul et al., 2011). From 1980 to

Table 1. Lithostratigraphic description, plant macrofossil composition of selected samples and inferred depositional environment for CP3.

Depth (m) below water surface	Lithostratigraphic description	Units	Composition of plant macro remains	Inferred depositional environment
2.00–2.02	Loose organic sediment	1	**Depth 2.20–2.23 m:**	Aquatic
2.02–2.04	Dark brown peat, compact		Occasional plant remains	
2.04–2.22	Dark brown fibrous peat			
2.22–2.73	Dark brown soft fibrous peat; loose soft peat between 2.33 and 2.68 m	2	**Depth 2.54–2.57 m:** Large pieces of aquatic plant remains (e.g. *Potamogeton*); Cyperaceae spp., *Typha* and Poaceae seeds.	Aquatic
			Depth 2.60–2.63 m: Woody fragments, plant remains, Cyperaceae spp., *Utricularia*, *Najas* and *Nymphoides indicum* seeds; macroscopic charcoal.	Aquatic–telmatic
			Depth 2.63–2.66 m: Plant remains; Cyperaceae spp., *Nympoides indicum*, *Typha* and Poaceae seeds; macroscopic charcoal.	Aquatic–telmatic
			Depth 2.66–2.69 m: Relatively high amount of plant remains, woody remains and Cyperaceae spp. and *Nymphoides indicum* seeds.	Telmatic–terrestrial
2.73–3.04	Dark brown compact peat	3	**Depth 2.73–2.78 m:** Plant remains and Poaceae seeds.	Telmatic–terrestrial
			Depth 2.98–3.04 m: Coarse organic material, e.g. large wood remains; charred plant remains and Cyperaceae spp. seeds.	Terrestrial
3.04–3.34	Dark brown peaty gyttja/coarse detritus gyttja with some fibrous peat horizons	4	**Depth 3.32–3.36 m:** Fine light roots and other plant remains; *Nymphaea*, Cyperaceae spp., *Typha*, *Scirpus*, *Utricularia* and Poaceae seeds.	Aquatic–telmatic
3.34–3.36	Transition zone between unit 5 and 4	5	**Depth 3.44–3.48 m:**	Aquatic
3.36–3.50	Dark brown fine detritus gyttja with some peaty horizons		Occasional plant remains	

2011, sub-decadal and decadal weakening of the summer monsoon in Thailand has also been associated with ENSO variability, specifically with the increasing number of El Niño events (Bridhikitti, 2013; Hsu et al., 2014; Singhrattna et al., 2005).

Prior reconstructions of the regional paleoenvironment based on pollen and spore studies from a 2.30 m long sequence of Lake Pa Kho (Penny, 1998, 2001) showed vegetation changes at the Pleistocene/Holocene transition (ca 12,000–10,000 cal yr BP), with the expansion of tropical and sub-tropical broad-leaf taxa in response to the development of relatively humid climatic conditions (Penny, 2001, 1998). However, this reconstruction (Penny, 1998, 2001) did not extend into the late-Holocene and did not provide information on hydroclimatic conditions and vegetation change after 5000 cal yr BP. The absence of late-Holocene sediments suggests that the earlier coring location either did not accumulate or did not preserve the most recent history of the site.

3. Materials and methods

During fieldwork in January 2010, two overlapping 10-m long sequences were cored in the central part of the southern basin (Figure 1B) using a modified Russian corer (7.5 cm diameter, 1 m length). The core sections were described in the laboratory, and each 1-m-long core segment was scanned with the Itrax XRF core scanner at 5 mm resolution using a Mo tube set at 30 kV and 30 mA for 60 s/point. Distinct lithological markers and ITRAX scanning results were used to correlate between parallel core segments, thus creating a composite stratigraphy for coring point CP3. The sequence of 2.00–3.50 m depth below the water surface is the focus of this study and was subdivided into five lithostratigraphic units (Table 1). Consecutive samples comprising 1-cm intervals were freeze-dried. The part between 3.50 and 11.00 m depth is still being analyzed (Chabangborn, 2014).

Selected elemental data (Si, K, and Ti) obtained from XRF scanning were averaged over 1 cm intervals and then normalized by (incoherent + coherent) scattering to remove various instrumental effects (Kylander et al., 2011). Si, K and Ti are here used as proxies for mineral input.

For further geochemical analyses, each freeze-dried and ground sample (150 samples in total) was weighed into a tin capsule for analysis with an elemental analyzer (Carlo Erba NC2500) connected to a Finnigan MAT Delta + mass spectrometer. Total organic carbon (TOC) and total nitrogen (TN) were measured in weight percentage, and their values are interpreted as productivity indicators. C/N ratios are expressed as atomic ratios. In lake sediments these ratios allow discrimination between aquatic and terrestrial organic matter sources (Meyer and Teranes, 2001; Meyers, 2003). In peatlands, however, C/N ratios may indicate changes in the type of peat-forming plants (Kuhry and Vitt, 1996) and/or are an indicator of the degree of peat decomposition (Chimner and Ewel, 2005). $\delta^{13}C_{org}$ values are reported in parts per thousand (permille, ‰) relative to the Vienna PeeDee Belemnite (VPDB, for C), with an analytical error of ±0.15‰, and are here used as a proxy for the contribution of aquatic versus terrestrial plants (Meyer and Teranes, 2001; Meyers, 2003).

To assess the productivity of siliceous microfossils, 51 samples were selected for analysis of biogenic silica (BSi) and pre-cleaned with H_2O_2 and HCl to remove organic matter and carbonate. The BSi content was determined by alkaline extraction of 30 mg of material in 40 mL of 1% Na_2CO_3 solution over a 5 h period, with sub-samples taken at 3 (within), 4 and 5 h and neutralized with 0.21 N HCl. The extracts were analyzed for dissolved silica (DSi) by ICP-OES (Varian Vista Ax), and the concentration data were plotted against depth/time. The easily soluble phases (e.g. diatom frustules, phytoliths) are dissolved within 2 h. Crystalline phases (silicate minerals) take a longer time to dissolve. Through calculating a linear regression between the 3, 4 and 5 h measurements of DSi values, we can differentiate the biogenic silica dissolved. The value where the linear regression crosses the vertical axis (the y-intercept) of the sub-sample plots was considered to be the BSi (wt %) corrected for a simultaneous dissolution of silica from minerals. Based on peaks in the BSi curve, 15 sub-samples were further

analyzed to estimate the relative contribution of diatoms and phytoliths. Much of the sample material had however already been used for other analyses; therefore the diatom/phytolith analyses are not continuous. Sub-samples for diatom and phytolith analysis were treated with 10% HCl to remove any carbonates and heated in H_2O_2 to oxidize organic matter. An aliquot of each sample was dried onto a cover slip, which was mounted onto a glass slide using a permanent mounting medium (Zrax or Naphrax).

The chronostratigraphy is based on 20 AMS ^{14}C ages (Table 2; Figure 2B and C). Sieve remains (mesh size 0.5 mm) of the samples were identified under a stereomicroscope and rinsed multiple times in deionized water. Samples with a sufficient amount of plant remains (charcoal, seeds, leaves, insects, and small wood fragments) were chosen for dating. The selected samples were dried overnight at 105 °C in pre-cleaned glass vials and sent to the [14]CHRONO Centre at Queen's University, Belfast for analysis. The sieve residues of 9 samples were further examined for macroscopic plant remains and charcoal. The plant assemblage types were described, and the depositional environment was classified as aquatic/open water, telmatic (larger plant fragments originating from e.g. reeds, sedges and horsetails), or terrestrial (Table 1, Figure 3).

The radiocarbon age and one standard deviation were calculated using the Libby half-life of 5568 years and a fractionation correction based on $\delta^{13}C$ measured on the AMS (Table 2). The age-model was constructed using Bacon, a Bayesian statistics-based routine that models accumulation rates by dividing a sequence into many thin segments and estimating the (linear) accumulation rate for each segment based on the (calibrated) ^{14}C dates, together with assumptions about accumulation rate and its variability between neighboring segments (Blaauw and Christen, 2011). Prior to selecting the present age models (CP3_82,

Table 2. [14]C dates for CP3. Core depth (in m) is given below the water surface. See Figure 1 for the location of the coring point. The stratigraphic units relate to those shown in Table 1.

Lab ID	Core depth (m)	[14]C date BP ± 1 σ	Dated material	Unit
UBA-23310	2.10–2.13	188 ± 24	*Scirpus*, *Nymphaea*, Cyperaceae seeds; charcoal, insects, wood piece	1
UBA-18074	2.20–2.23	299 ± 23	Seeds*, charcoal, insects	1
UBA-14635	2.54–2.57	410 ± 38	Seeds*, charcoal, wood	2
UBA-18075	2.57–2.60	434 ± 23	Seeds*, charcoal, wood	2
UBA-23756	2.60–2.63	638 ± 31	*Nymphaea* seeds, charcoal, charred plant remains, wood, bark, insects	2
UBA-19839	2.60–2.63	687 ± 23	Seeds*	2
UBA-14636	2.63–2.66	1153 ± 26	Seeds*, charcoal, wood	2
UBA-12777	2.70–2.73	1388 ± 22	Plant remains*	2
UBA-19840	2.70–2.73	1312 ± 25	Seeds*, insects, leaf fragments*	2
UBA-23311	2.73–2.78	1459 ± 28	*Nymphaea*, Cyperaceae seeds; charcoal, insects, leaf fragments*	3
UBA-23312	2.78–2.83	1777 ± 34	*Nymphaea*, Cyperaceae seeds; charcoal, wood, leaf fragment*	3
UBA-23313	2.83–2.88	1587 ± 25	*Nymphaea*, *Scirpus*, Cyperaceae seeds; charcoal, insects, leaf fragments*	3
UBA-18076	2.88–2.93	1602 ± 24	Seeds*, charcoal, insects	3
UBA-14637	2.93–2.98	1611 ± 21	Charcoal	3
UBA-19837	3.10–3.13	1625 ± 25	Seeds*, insects, leaf fragments*	4
UBA-18077	3.30–3.33	1822 ± 28	Seeds*, insects, leaf fragments*	4
UBA-14639	3.40–3.44	1873 ± 32	Small wood fragments	5
UBA-19841	3.40–3.44	2465 ± 29	Seeds*, leaf fragments, charcoal	5
UBA-16756	3.44–3.48	2083 ± 25	Seeds*, charcoal, wood, leaf fragments*	5
UBA-23283	3.48–3.52	2050 ± 28	Small wood fragments, plant remains*	5

* = Undetermined.

CP3_82_hiatus) (Figure 2B and C), multiple model runs were performed using different assumptions and parameters.

4. Results

4.1. Chronology

The ^{14}C dates for CP3 plot sequentially according to depth, but two ^{14}C dates (UBA-19841 at 3.40–3.44 m and UBA-23312 at 2.78–2.83 m) have older ages than expected (Table 2, Figure 2B and C) and are treated as outliers by Bacon. Sequential samples UBA-14636 (2.66–2.63 m) and UBA-19839 (2.63–2.60 m) differ in age by c 460 calibrated ^{14}C years (Table 2). Explanations for this age difference between adjoining levels include low accumulation rates or the presence of a hiatus. The stratigraphy, TOC, C/N ratio, elemental data and plant macrofossil composition give no indication for an abrupt change or a hiatus at 2.63 m depth, but $\delta^{13}C$ and BSi values show a distinct shift (Table 1; Figure 3).

We therefore constructed two age models; one assuming low accumulation rates (CP3_82) around 2.63 m, and one assuming the presence of a hiatus (CP3_82_hiatus) (Figure 2B and C). Both age models provide similar ages for the sequence below 2.68 m depth and above 2.63 m depth, but result in a different duration (510 and 170 years, respectively) for the depth interval between 2.68 and 2.63 m. Lower accumulation rates between 2.68 and 2.63 m (AD 840–1320) as shown in the age model of CP3_82 (Figure 2B) are inconsistent with the deposition of fibrous and less decomposed peat. The $\delta^{13}C_{org}$ values of −22 to 23‰ and occurrence of aquatic–telmatic plants also suggest the availability of water and conditions favorable for peat accumulation (Figure 3). Age model CP3_82_hiatus on the other hand implies continuous accumulation between 2.68 and 2.63 m depth (AD 800–970), followed by a 330 year long hiatus (Figure 2 C). Since peat accumulation below and above 2.63 m depth occurred at a similar rate in both age models, a sudden slowdown in accumulation rate between 2.68 and 2.63 m, at the same time as $\delta^{13}C_{org}$ increase and plant remains suggest wetland conditions, seems difficult to reconcile. Our preferred hypothesis is therefore to include a hiatus at 2.63 m depth.

4.2. Stratigraphy and geochemistry of Pa Kho

The stratigraphy of CP3 shows from bottom to top a fine detritus gyttja, peaty gyttja, peat and loose organic sediments (Table 1). The overall high TOC content of the sequence suggests high organic production (Figure 3).

$\delta^{13}C_{org}$ values (−24 to −21‰) in the lowermost fine detritus and peaty gyttja (3.50–3.04 m depth; BC 170–AD 370) indicate that the sediments contain a mix of aquatic, telmatic and terrestrial organic material (Figure 3). Macroscopic plant remains and the presence of diatoms and phytoliths would support this. C/N ratios of 27–24, however, point to a predominantly terrestrial organic carbon source (Meyer and Teranes, 2001; Meyers, 2003) and suggest, together with elevated values for Si, K, and Ti, that run-off was important. Taken together, the proxy data indicate that Pa Kho was a shallow productive lake or a wetland with areas of open water between BC 170 and AD 370.

The transition from peaty gyttja to compact peat at AD 370 coincides with a distinct decrease in $\delta^{13}C_{org}$ values from −23 to −28‰, an increase in BSi (phytoliths) and the occurrence of terrestrial plant remains (Figure 3). $\delta^{13}C_{org}$ values remain low between 3.04 and 2.98 m (AD 370–410), increase again to −24‰ between 2.98 and 2.93 m (AD 410–450), and display low, but fluctuating values of −30 to −27‰ until 2.68 m (AD 800). The overall gradual decrease in the C/N ratio, which
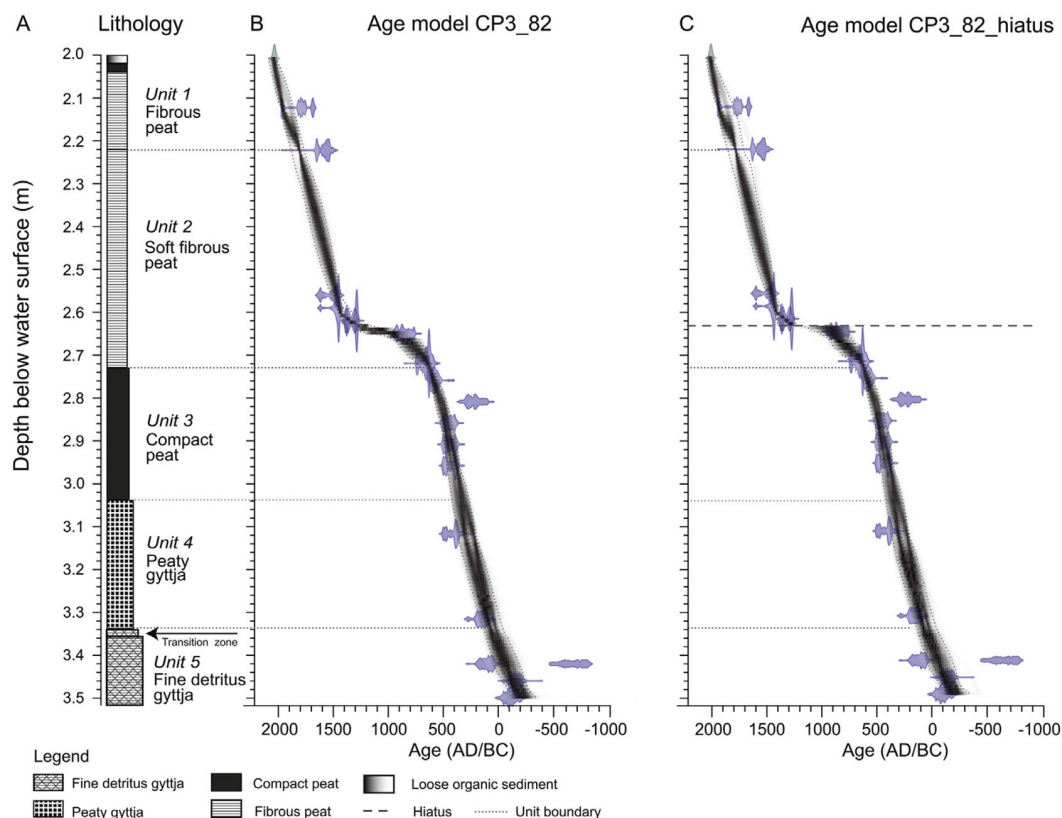
Figure 2. (A) Lithostratigraphy for CP3, (B) age model CP3_82 and (C) age model CP3_82_hiatus. The blue shapes show the calibrated ^{14}C dates with two standard deviations, the grey shading indicates the likely age model and the dotted lines show the 95% confidence ranges of the age model. See Table 1 for a detailed description of the sequence and Table 2 for the ^{14}C dates.

starts at 2.93 m (AD 450), may be explained by peat decomposition. This process liberates soluble carbon compounds, whereas nitrogen remains relatively constant, because most of its labile forms have already been consumed or transformed to inorganic forms (Chimner and Ewel, 2005; Ise et al., 2008). Charcoal was observed between 2.98 and 2.73 m (AD 410–650), and the sample analyzed for plant remains between 2.78 and 2.73 m (AD 580–650) is composed of terrestrial-telmatic species (Figure 3). The different proxies thus suggest the development of a peatland between AD 370 and 800, but also that conditions may have been variable, with a lower water table and lower effective moisture between AD 370 and 410 and between AD 450 and 800, and slightly higher moisture availability between AD 410 and 450.

The marked increase in $\delta^{13}C_{org}$ values to −21‰ at 2.68 m and the shift from terrestrial–telmatic to telmatic–aquatic plant assemblages at 2.66 m (Figure 3) point to the re-establishment of a wetland at Pa Kho, and thus to higher effective moisture between AD 800 and 970. The subsequent hiatus suggested by the age model (CP_82_hiatus) at 2.63 m depth implies that 330 years are 'missing' in our record. Such a gap in a peat sequence can be caused by decomposition and oxidation of the organic material under aerobic conditions. Although the different processes affecting tropical peatlands are still poorly understood, a recent laboratory experiment shows that drought can lead to considerable carbon loss in tropical peat samples (Fenner and Freeman, 2011). Indeed, the lowest $\delta^{13}C_{org}$ values (−28‰) and the peak in BSi (phytoliths) just above the hiatus, i.e. between 2.63 and 2.62 m (AD 1300–1340) (Figure 3), suggest an expansion of terrestrial plants onto the former wetland and generally lower effective moisture, which persisted until 2.58 m (AD 1450). In contrast, the telmatic–aquatic plant assemblage

between 2.63 and 2.60 m points to a water-saturated peat surface. This discrepancy can, however, be explained by the fact that each geochemical sample covers a 1-cm interval, while the macrofossil sample corresponds to a 3-cm interval and thus incorporates a mixed signal (Figure 3). A lower and/or fluctuating water table would have led to exposure of the peat surface, and consequently to oxidation and/or biodegradation of the underlying organic material that had been accumulating between AD 970 and 1300.

The gradual increase in $\delta^{13}C_{org}$ values to −22‰ after AD 1450 (Figure 3) and the macroscopic plant remains show that telmatic–aquatic plant material contributed to the organic carbon pool. $\delta^{13}C_{org}$ values remain constant (−24 and −25‰) between 2.51 and 2.02 m (AD 1510–2001), and the presence of the diatom species *Eunotia yanomami*, *Eunotia incisa*, *Eunotia intermedia*, *Eunotia monodon*, and *Gomphonema gracile* coupled with the plant macrofossil composition indicate a wetland environment.

The stepwise increase in BSi content at 2.31 m (AD 1700) and 2.07 m depth (AD 1960) may signify higher nutrient availability, and the distinct increase in major elements (Si, K, Ti) at 2.17 m depth (AD 1850) and at 2.05 m depth (AD 1970) is likely related to land-use changes around Pa Kho (Klubseang, 2011). This would suggest a significant human impact, which overprints any climate signal. The historical record around the region is not well documented, but the change seen in the Pa Kho's sequence after AD 1700 coincides with the start of agricultural intensification in SE Asia (Lieberman and Buckley, 2012). The high C/N ratio (22), high $\delta^{13}C$ values (−22‰) and peaks of BSi, diatom and elemental data (Si, K, Ti) during the last 10 years are likely the result of the dam and intensified cultivation around the lake.
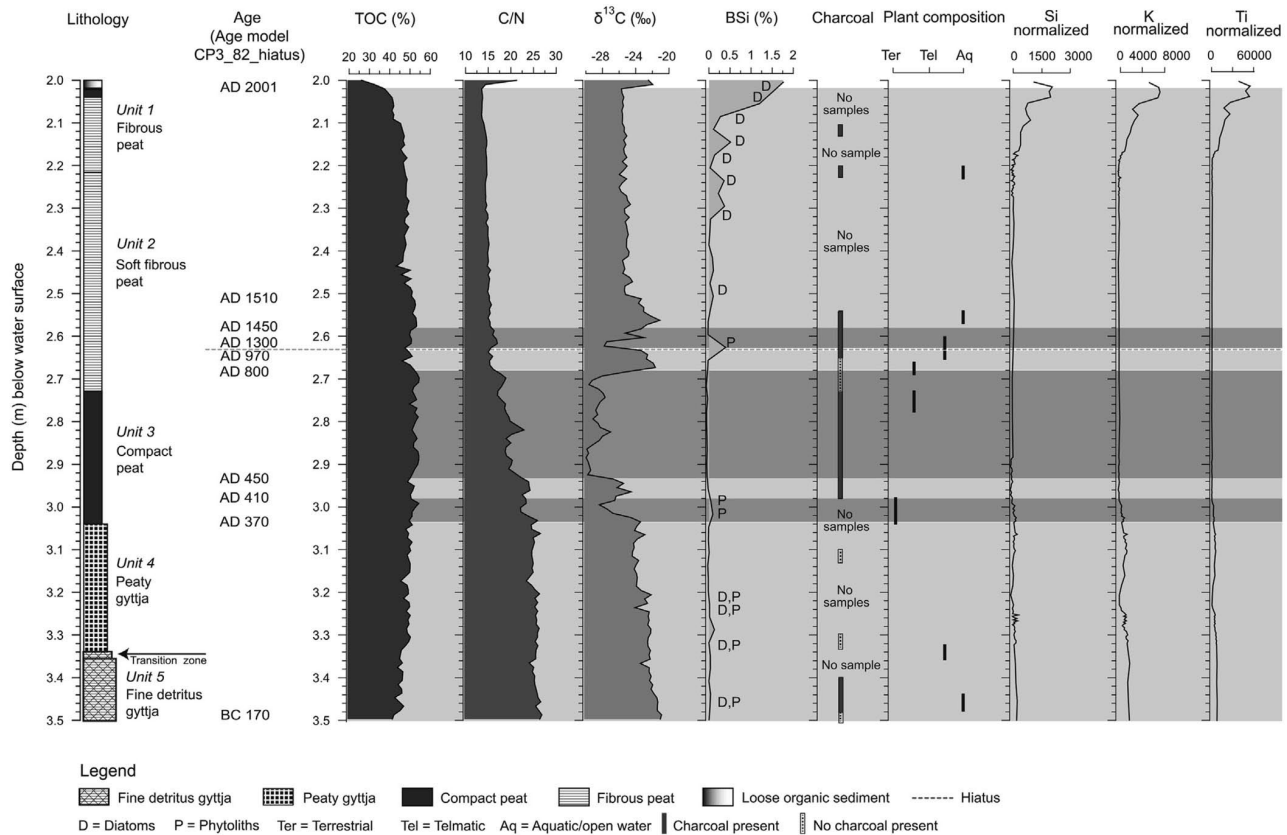
Figure 3. Lithostratigraphy, geochemistry, and selected elemental data for CP3. The samples analyzed for diatoms, phytoliths, charcoal, and plant macrofossil composition are discontinuous (see text for further explanations). Light gray bars represent higher effective moisture, and the dark gray bars represent lower effective moisture.

5. Discussion

The sedimentary proxies show that Pa Kho was a shallow productive lake or wetland between BC 170 and AD 370. Such an environment implies high effective moisture, likely caused by a strengthened summer monsoon. Around AD 370 the wetland transformed to a peatland with a lower water table, which suggests a decrease in effective moisture and a weakening of the summer monsoon. This transition occurred in a stepwise fashion, given that alternating intervals of lower effective moisture (AD 370–410), slightly higher effective moisture (AD 420–450) and lower effective moisture (until AD 800) are inferred (Figure 4c). The re-establishment of a wetland between AD 800 and 970 is a sign of higher effective moisture and likely reflects increased summer monsoon precipitation. The subsequent hiatus (AD 970–1300) might have been caused by degradation of the peat surface during an interval with lower effective moisture and a weakened summer monsoon (AD 1300–1450) (Figure 4c). The increase in aquatic plant remains, the appearance of diatoms and the isotope proxies show again a wetland environment starting around AD 1450. This marks a return to higher effective moisture and a moderately strengthened summer monsoon. The geochemical proxies established for CP3 can be compared with the multi-sediment and multi-proxy records of Lake Kumphawapi, which is located 15 km to the northeast. These showed the re-establishment of a shallow lake around AD 150–350 and suggested higher effective moisture and a strengthened summer monsoon (Chawchai et al., 2013; Wohlfarth et al., 2012), similar to our interpretation of the Pa Kho record. However, a detailed interpretation of the

paleoenvironment in Kumphawapi after AD 350 is limited due to chronological uncertainties.

Given the lack of paleo-precipitation records from tropical lakes and wetland in Southeast Asia, it is important to examine whether the environmental signals stored in Pa Kho's sequence are a reflection of summer monsoon variability. To infer spatial patterns of hydroclimatic variability, we compare the Pa Kho data set to selected high-resolution paleoclimatic records established for the Asian monsoon region. The stronger/weaker summer monsoon intervals presented in Figure 4a–f follow the interpretation of the respective authors and present a fairly coherent picture of Asian summer monsoon variability. The terrestrial plant leaf wax (δD_{wax}) record established from marine sediments from the Makassar Strait, Southwest Sulawesi (Tierney et al., 2010) is the only high-resolution record extending as far back as Pa Kho, while the Wanxiang Cave $\delta^{18}O$ data set commences around AD 200 (Zhang et al., 2008). All other high-resolution records only cover the last 1400 years (central India composite record) (Berkelhammer et al., 2010; Sinha et al., 2011a, 2011b, 2007); the last 1000 years (Dongdao Island) (Yan et al., 2011) or the past 700–800 years (MADA data set; Dayu Cave) (Buckley et al., 2007, 2010, 2014; Cook et al., 2010; Tan et al., 2009) (Figure 4a–f).

Higher effective moisture (BC 170–AD 370), followed by a stepwise decline (AD 370–450) and lower moisture availability (AD 450–800) as reconstructed for Pa Kho is comparable with the $\delta^{18}O$ record from Wanxiang Cave in central China (Figure 4a and c). This record suggests that the summer monsoon was moderately strong between AD 190–530, gradually declined after AD 530 and was markedly weaker between AD 860–940 (Zhang et al., 2008) (Figure 4a and c).
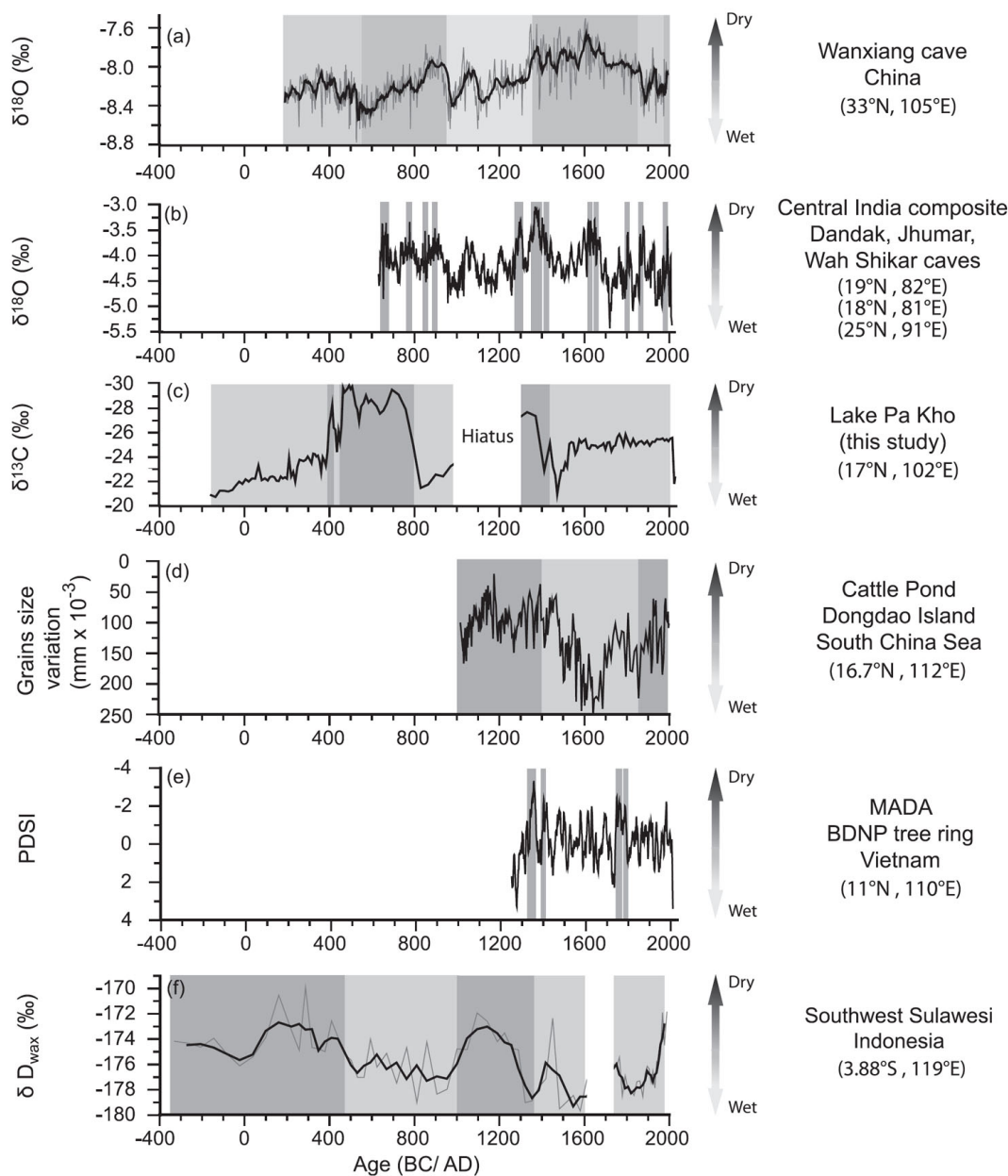
Figure 4. Selected high-resolution records for the Asian monsoon region for the past 2000 years: (a) δ¹⁸O data of Wanxiang Cave speleothems (Zhang et al., 2008); (b) Composite δ¹⁸O time series for central India based on speleothems from Dandak, Jhumar, and Wah Shikar Caves (Berkelhammer et al., 2010; Sinha et al., 2011a, 2011b, 2007); (c) δ¹³C$_{org}$ data from Lake Pa Kho (this study); (d) grain size variations in sediment core DY6-MGS of Cattle Pond, Dongdao Island (Yan et al., 2011); (e) Palmer Drought Severity Index (PDSI) derived from the Monsoon Asia Drought Atlas (MADA) for the region between 10 and 20°N and 95–115°E (Buckley et al., 2007, 2010, 2014; Cook et al., 2010; D'Arrigo et al., 2011; Sano et al., 2009); (f) δD$_{wax}$ from marine cores 31 MC and 34 GGC from southwest Sulawesi (Tierney et al., 2010). The vertical light gray bars represent higher effective moisture/a strengthened summer monsoon, and the dark gray bars represent lower effective moisture/a weakened summer monsoon. Note that the timing of the shifts in moisture history of the individual records follows that cited by the respective author/s. See Figure 5 for the location of the different records.

The offset of 60–140 years between the two data sets at the beginning and end of the weaker summer monsoon period, respectively, may stem from chronological uncertainties. Upwelling indicators *(Globigerina bulloides)* in sediments from the northwestern Arabian Sea also show a weakening of the summer monsoon starting around AD 450 (Anderson et al., 2010, 2002), and the composite speleothem δ¹⁸O records from Indian caves give evidence for decadal intervals of a distinctly weaker summer monsoon between AD 650–900 (Berkelhammer et al., 2010; Sinha et al., 2011a, 2007) (Figure 4b). These time intervals of a stronger/weaker Asian summer monsoon, however, differ from to the δD$_{wax}$ record from the Makassar Strait (Figure 4 a–c and f), which suggests a weaker Asian monsoon until around AD 450 and subsequently a stronger monsoon until about AD 1000 (Tierney et al., 2010) (Figure 4f).

Berkelhammer et al., 2010, Sinha et al., 2011a and Sinha et al., 2007 and Zhang et al. (2008) infer a strengthening of the summer monsoon between AD 950–1300 from speleothem δ¹⁸O records (Figure 4a and b). These findings are comparable

within error margins to our data set, which suggests higher effective moisture starting around AD 800 (Figure 4c), but they differ from lower precipitation inferred over Dongdao Island in the South China Sea between AD 1000–1400 (Yan et al., 2011) (Figure 4d). δD$_{wax}$ values from the Makassar Strait also imply a weaker summer monsoon throughout the period AD 1000–1350 (Tierney et al., 2010) (Figure 4f).

The Pa Kho data set gives evidence for distinctly lower effective moisture between AD 1300 and 1450. This coincides, within error margins, with the start of a weaker summer monsoon phase recorded in Wanxiang Cave (Zhang et al., 2008) (Figure 4a), and also compares to the intervals of lower precipitation (AD 1249–1325; 1390–1420) inferred from speleothem δ¹⁸O values in Dayu Cave (Tan et al., 2009). Decreased upwelling in the Arabian Sea (AD 1350–1550) is also interpreted as a weakening of the Asian summer monsoon (Anderson et al., 2010, 2002). Distinct decadal-long droughts are recognized in the δ¹⁸O records of Indian cave speleothems between AD 1300–1450 (Berkelhammer et al., 2010; Sinha et al.,
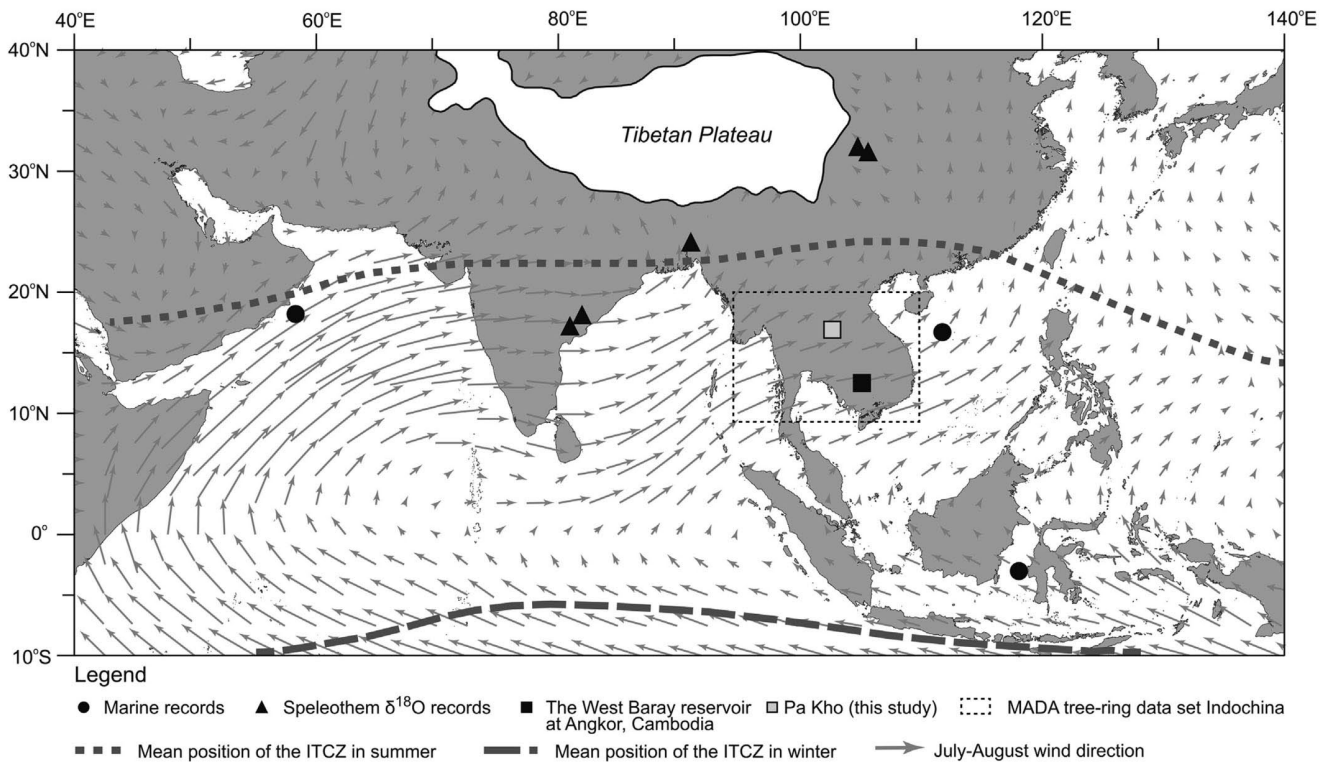
Figure 5. Location of selected high-resolution Asian monsoon paleo-records for the last 2000 years. The mean position of the winter and summer Intertropical Convergence Zone (ITCZ) is according to Wang (2009). The July–August wind directions and wind speeds follow Wang et al. (2003). Long arrows indicate high wind speed and short arrows lower wind speed.

2011a, 2011b, 2007), in the MADA tree-ring data set (AD 1340–1370; 1400–1425) and in the sediment proxies from the West Baray reservoir at Angkor, Cambodia (AD 1300–1400) (Buckley et al., 2007, 2010; Cook et al., 2010; Day et al., 2012) (Figure 4b and e). The Dongdao Island (Yan et al., 2011; Yan et al., 2011) and Makassar Strait (Tierney et al., 2010) records on the other hand imply a shift towards a strengthened summer monsoon around AD 1350–1400 (Figure 4d and f).

The inferred moisture history for Pa Kho since AD 1450 (Figure 4c) compares well to the moderately intense summer monsoon reconstructed from Indian cave speleothems (Berkelhammer et al., 2010; Sinha et al., 2011a, 2011b, 2007) and Arabian Sea proxies (Anderson et al., 2010, 2002), but seems to diverge from the hydroclimatic scenario established for Wanxiang Cave (Zhang et al., 2008). A correspondence can also be found between the Pa Kho record and climate inferences for Dongdao Island and southwest Sulawesi, where higher precipitation has been reconstructed since AD 1400 (Figure 4d and f) (Tierney et al., 2010; Yan et al., 2011). It is interesting, however, to note that the interpretation of the speleothem δ^{18}O records from Wanxiang Cave (Zhang et al., 2008) and neighboring Dayu Cave (Tan et al., 2009) do not correspond to each other. For Wanxiang Cave, a generally weaker summer monsoon is reconstructed throughout the time interval AD 1350–1850 (Zhang et al., 2008), whereas the Dayu Cave record suggests a weaker summer monsoon around AD 1300–1400, an increase in summer monsoon intensity around AD 1500, intervals of higher monsoon precipitation between AD 1535–1685, AD 1755–1835 and AD 1920–1970, and lower precipitation between AD 1890 and 1915 (Tan et al., 2009). When Li et al. (2014) compared speleothem δ^{18}O records from a region spanning from 60° to 125°E and from 10° to 40° N, they observed similar and divergent precipitation patterns in close-by speleothem records from China. This would suggest that monsoon

precipitation on decadal and centennial time scales varied regionally and that the response to climate change between and within each monsoon sub-system is complicated. The obvious differences between the two speleothem data sets starting around AD 1500 would imply that speleothem δ^{18}O values do not provide a straightforward measure for large-scale regional summer monsoon intensity, but that they also record sub-regional precipitation signals, or that a number of other factors are involved in creating the δ^{18}O signal (Li et al., 2014).

Sinha et al., 2011a and Sinha et al., 2011b note a distinct shift in precipitation patterns around AD 1650–1700, when δ^{18}O values from caves in northern and central India start to diverge. Records from central India suggest a shift from drier to wetter conditions, while the northern Indian caves indicate a shift from wetter to drier conditions. This shift in precipitation patterns has been interpreted as reflecting active and break phases of the Indian summer monsoon (Sinha et al., 2011a). The decadal droughts during the 17th and 18th centuries registered in Indian cave speleothems (Berkelhammer et al., 2010; Sinha et al., 2011a, 2011b, 2007) and in the MADA data set (Buckley et al., 2007, 2010, 2014; Cook et al., 2010; D'Arrigo et al., 2011; Sano et al., 2009) are not recognized in the Pa Kho proxies (Figure 4b–e). This is likely due to the lower temporal resolution as compared to the tree-ring and speleothem records, but it could also be that human impact overprinted any climatic signals.

The opposing hydroclimatic patterns seen between Wanxiang Cave and Pa Kho in the north and southwest Sulawesi in the south can be explained by their location relative to the migration of the ITCZ (Sinha et al., 2011b; Tierney et al., 2010), and by interactions between the Asian-Australian monsoon systems. A strengthened Asian summer monsoon between BC 170–AD 500 and between AD 900–1300, in combination with a weak Australian monsoon, would have led to a shift of the tropical rain belt northward of Indonesia, leading to drought

in equatorial regions. The opposite would have been the case between AD 500–900 and between AD 1300–1450, when the Asian summer monsoon weakened and the mean position of the tropical rain belt shifted over Indonesia. This hydroclimatic scenario seems to have changed after AD 1450, when the two neighboring Chinese cave records show opposing dry/wet patterns, the northeast Indian cave speleothems a shift to dry conditions and the central Indian caves a shift to wetter condition, while Pa Kho shows patterns similar to those on Dongdao Island and in Southwest Sulawesi (Figure 4a–f). Independent of the differences between Wanxiang and Dayu Caves, which could stem from local factors, we may assume that the effect of a moderately strengthened summer monsoon was only registered as far north as 20° N, while rainfall was strong over the equatorial region. We thus hypothesize that the mean summer position of the ITCZ over land did not reach as far north as during the strengthened summer monsoon intervals before AD 1450 and that it was located approximately where it is today (Figure 5). Similar conclusions have been drawn based on a record from the central equatorial Pacific (Sachs et al., 2009).

Decadal drought intervals during the past 700–800 years seen in the in the MADA tree ring data series and in Dayu Cave speleothems have been linked to ENSO variability (Cook et al., 2010; Tan et al., 2009). However, the moisture history derived from Wanxiang Cave has been associated with solar influence and climate variability in the North Atlantic region (Zhang et al., 2008). Decadal drought observed in the Indian speleothems, on the other hand, has been linked to Indian Ocean variability (Sinha et al., 2011a, 2011b). The centennial-scale shifts in hydroclimatic conditions reconstructed for Pa Kho support shifts in the mean position of the ITCZ as these produced associated changes in summer monsoon precipitation. IOD and ENSO events also may have had important influences on monsoon rainfall on decadal time scales, but these are not clearly registered in our centennial-scale record.

A more precise reconstruction of the temporal and spatial variability of past monsoon precipitation patterns and their underlying causes would require several additional high-resolution hydroclimatic records from the Asian monsoon region. Only a dense network of well-dated, multi-proxy data sets can help to reduce the current uncertainties in interpretation and provide a valid base for evaluating the inherent leads and lags of different proxies used to infer hydroclimatic conditions.

6. Conclusions

The new hydroclimatic reconstruction based on the high-resolution data set established for Lake Pa Kho in northeast Thailand adds important information in data coverage between China and Indonesia during the last two millennia. The multi-proxy study of the Pa Kho sequence reveals time intervals when the summer monsoon was strengthened (BC 170–AD 370, AD 800–960, and since AD 1450) and time intervals of drought (AD 370–800 and AD 1300–1450). Within error margins the effective moisture variability (BC 170–AD 1450) reconstructed for Pa Kho is comparable to hydroclimatic patterns derived from speleothem proxies in China and India. The drought intervals expressed in these records compare to intervals of stronger monsoonal rainfall in equatorial regions, as shown by the record from the Makassar Strait in Indonesia. This hydroclimatic pattern seems to have changed sometime between AD 1450–1600, when the inferred moisture history for Pa Kho became more similar to that reconstructed for the South China Sea and the Indonesian region. This would

suggest that the mean position of the ITCZ over land generally did not reach as far north as it did prior to AD 1450.

References

Anderson, D.M., Baulcomb, C.K., Duvivier, A.K., Gupta, A.K., 2010. Indian summer monsoon during the last two millennia. J. Quat. Sci. 25, 911– 917. doi: 10.1002/jqs.1369.

Anderson, D.M., Overpeck, J.T., Gupta, A.K., 2002. Increase in the Asian Southwest Monsoon during the past four centuries. Science 297, 596– 599. doi: 10.1126/science.1072881.

Berkelhammer, M., Sinha, A., Mudelsee, M., Cheng, H., Edwards, R.L., Cannariato, K., 2010. Persistent multidecadal power of the Indian Summer Monsoon. Earth Planet. Sci. Lett. 290, 166– 172. doi: 10.1016/j.epsl.2009.12.017.

Blaauw, M., Christen, J., 2011. Flexible paleoclimate age-depth models using an autoregressive gamma process. Bayesian Anal. 6, 457– 474.

Bridhikitti, A., 2013. Connections of ENSO/IOD and aerosols with Thai rainfall anomalies and associated implications for local rainfall forecasts. Int. J. Climatol. 33, 2836– 2845. doi: 10.1002/joc.3630.

Buckley, B., Palakit, K., Duangsathaporn, K., Sanguantham, P., Prasomsin, P., 2007. Decadal scale droughts over northwestern Thailand over the past 448 years: Links to the tropical Pacific and Indian Ocean sectors. Clim. Dyn. 29, 63– 71. doi: 10.1007/s00382-007-0225-1.

Buckley, B.M., Anchukaitis, K.J., Penny, D., Fletcher, R., Cook, E.R., Sano, M., Nam, L.C., Wichienkeeo, A., Minh, T.T., Hong, T.M., 2010. Climate as a contributing factor in the demise of Angkor, Cambodia. Proc. Natl. Acad. Sci. 107, 6748– 6752. doi: 10.1073/pnas.0910827107.

Buckley, B.M., Fletcher, R., Wang, S.-Y.S., Zottoli, B., Pottier, C., 2014. Monsoon extremes and society over the past millennium on mainland southeast Asia. Quat. Sci. Rev. 95, 1– 19. doi: 10.1016/j.quascirev.2014.04.022.

Chabangborn, A., 2014. Asian Monsoon Over Mainland Southeast Asia in the Past 25000 Years (PhD thesis). Stockholm University, Stockholm, Sweden, 65 pp.

Chawchai, S., Chabangborn, A., Kylander, M., Löwemark, L., Mörth, C.-M., Blaauw, M., Klubseang, W., Reimer, P.J., Fritz, S.C., Wohlfarth, B., 2013. Lake Kumphawapi—An archive of Holocene palaeoenvironmental and palaeoclimatic changes in northeast Thailand. Quat. Sci. Rev. 68, 59– 75. doi: 10.1016/j.quascirev.2013.01.030.

Chimner, R.A., Ewel, K.C., 2005. A tropical freshwater wetland: II. Production, decomposition, and peat ormation. Wetl. Ecol. Manag. 13, 671– 684. doi: 10.1007/s11273-005-0965-9.

Cobb, K.M., Charles, C.D., Cheng, H., Edwards, R.L., 2003. El Niño/ Southern Oscillation and tropical Pacific climate during the last millennium. Nature 424, 271– 276. doi: 10.1038/nature01779.

Cook, E.R., Anchukaitis, K.J., Buckley, B.M., D'Arrigo, R.D., Jacoby, G.C., Wright, W.E., 2010. Asian Monsoon failure and megadrought during the Last Millennium. Science 328, 486– 489. doi: 10.1126/science.1185188.

D'Arrigo, R., Palmer, J., Ummenhofer, C.C., Kyaw, N.N., Krusic, P., 2011. Three centuries of Myanmar monsoon climate variability inferred from teak tree rings. Geophys. Res. Lett. 38, L24705. doi: 10.1029/2011GL049927.

Day, M.B., Hodell, D.A., Brenner, M., Chapman, H.J., Curtis, J.H., Kenney, W.F., Kolata, A.L., Peterson, L.C., 2012. Paleoenvironmental

history of the West Baray, Angkor (Cambodia). Proc. Natl. Acad. Sci. 109, 1046– 1051. doi: 10.1073/pnas.1111282109.

El Tabakh, M., Utha-Aroon, C.,Warren, J.K., Schreiber, B.C., 2003. Origin of dolomites in the cretaceous Maha Sarakham evaporites of the Khorat Plateau, northeast Thailand. Sediment. Geol. 157, 235– 252. doi: 10.1016/S0037-0738(02)00235-X.

Fenner, N., Freeman, C., 2011. Drought-induced carbon loss in peatlands. Nat. Geosci. 4, 895– 900. doi: 10.1038/ngeo1323.

Hsu, H.-H., Zhou, T., Matsumoto, J., 2014. East Asian, Indochina and western North Pacific summer monsoon — An update. Asia-Pac. J. Atmos. Sci. 50, 45– 68. doi: 10.1007/s13143-014-0027-4.

Ise, T., Dunn, A.L., Wofsy, S.C., Moorcroft, P.R., 2008. High sensitivity of peat decomposition to climate change through water-table feedback. Nat. Geosci. 1, 763– 766. doi: 10.1038/ngeo331.

Klubseang, W., 2011. Paleogeography and Paleoenvironment of Nong Han Kumphawapi, Changwat Udon Thani (MSc thesis). Chulalongkorn University, Bangkok, pp. 1– 110.

Kuhry, P., Vitt, D.H., 1996. Fossil carbon/nitrogen ratios as a measure of peat decomposition. Ecology 77, 271– 275. doi: 10.2307/2265676.

Kylander, M.E., Ampel, L., Wohlfarth, B., Veres, D., 2011. High-resolution X-ray fluorescence core scanning analysis of Les Echets (France) sedimentary sequence: New insights from chemical proxies. J. Quat. Sci. 26, 109– 117. doi: 10.1002/jqs.1438.

Li, Y.,Wang, N., Zhou, X., Zhang, C.,Wang, Y., 2014. Synchronous or asynchronous Holocene Indian and East Asian summer monsoon evolution: a synthesis on Holocene Asian summer monsoon simulations, records and modern monsoon indices. Glob. Planet. Change 116, 30– 40. doi: 10.1016/j.gloplacha.2014.02.005.

Lieberman, V., Buckley, B., 2012. The impact of climate on Southeast Asia, circa 950–1820: New findings. Mod. Asian Stud. 1– 48. FirstView.

Limsakul, A., Paengkaew, W., Kummueang, A., Limjirakan, S., Suttamanuswong, B., 2011. PDSI-based variations of droughts and wet spells in Thailand: 1951– 2005. Environ. Asia 4, 12– 20.

Mann, M.E., Zhang, Z., Rutherford, S., Bradley, R.S., Hughes, M.K., Shindell, D., Ammann, C., Faluvegi, G., Ni, F., 2009. Global signatures and dynamical origins of the Little Ice Age and Medieval Climate Anomaly. Science 326, 1256– 1260. doi: 10.1126/science.1177303.

Meyer, P.A., Teranes, J., 2001. Sediment organic matter. In: Last, W.M., Smol, J.P. (eds.), Tracking Environmental Change Using Lake Sediments: Physical and Geochemical Methods. Dordrecht.

Meyers, P.A., 2003. Applications of organic geochemistry to paleolimnological reconstructions: A summary of examples from the Laurentian Great Lakes. Org. Geochem. 34, 261– 289. doi: 10.1016/S0146-6380(02)00168-7.

Newton, A., Thunell, R., Stott, L., 2006. Climate and hydrographic variability in the Indo-Pacific Warm Pool during the last millennium. Geophys. Res. Lett. 33, L19710. doi: 10.1029/2006GL027234.

Oppo, D.W., Rosenthal, Y., Linsley, B.K., 2009. 2,000-year-long temperature and hydrology reconstructions from the Indo-Pacific warm pool. Nature 460, 1113– 1116. doi: 10.1038/nature08233.

Pages 2K, Consortium, 2013. Continental-scale temperature variability during the past two millennia. Nat. Geosci. 6, 339– 346. doi: 10.1038/ngeo1797.

Penny, D., 1998. Late Quaternary Palaeoenvironments in the Sakon Nakhon Basin,North-East Thailand (PhD thesis). Monash University, Victoria/Australia, 260 pp.

Penny, D., 2001. A 40,000 year palynological record from north-east Thailand; implications for biogeography and palaeo-environmental reconstruction. Palaeogeogr. Palaeoclimatol. Palaeoecol. 171, 97– 128. doi: 10.1016/S0031-0182(01)00242-5.

Prasad, S., Anoop, A., Riedel, N., Sarkar, S., Menzel, P., Basavaiah, N., Krishnan, R., Fuller, D., Plessen, B., Gaye, B., R€ohl, U., Wilkes, H., Sachse, D., Sawant, R., Wiesner, M.G., Stebich, M., 2014. Prolonged monsoon droughts and links to Indo-Pacific warm pool: A Holocene record from Lonar Lake, central India. Earth Planet. Sci. Lett. 391, 171– 182. doi: 10.1016/j.epsl.2014.01.043.

Sachs, J.P., Sachse, D., Smittenberg, R.H., Zhang, Z., Battisti, D.S., Golubic, S., 2009. Southward movement of the Pacific intertropical convergence zone AD 1400–1850. Nat. Geosci. 2, 519– 525. doi: 10.1038/ngeo554.

Sano, M., Buckley, B.M., Sweda, T., 2009. Tree-ring based hydroclimate reconstruction over northern Vietnam from Fokienia Hodginsii: Eighteenth century mega-drought and tropical Pacific influence. Clim. Dyn. 33, 331– 340. doi: 10.1007/s00382-008-0454-y.

Singhrattna, N., Rajagopalan, B., Kumar, K.K., Clark, M., 2005. Interannual and interdecadal variability of Thailand summer monsoon season. J. Clim. 18, 1697– 1708. doi: 10.1175/JCLI3364.1.

Sinha, A., Berkelhammer, M., Stott, L., Mudelsee, M., Cheng, H., Biswas, J., 2011a. The leading mode of Indian summer monsoon precipitation variability during the last millennium. Geophys. Res. Lett. 38 doi: 10.1029/2011GL047713.

Sinha, A., Cannariato, K.G., Stott, L.D., Cheng, H., Edwards, R.L., Yadava, M.G., Ramesh, R., Singh, I.B., 2007. A 900-year (600 to 1500 A.D.) record of the Indian Summer Monsoon precipitation from the core monsoon zone of India. Geophys. Res. Lett. 34, L16707. doi: 10.1029/2007GL030431.

Sinha, A., Stott, L., Berkelhammer, M., Cheng, H., Edwards, R.L., Buckley, B., Aldenderfer, M., Mudelsee, M., 2011b. A global context for megadroughts in monsoon Asia during the past millennium. Quat. Sci. Rev. 30, 47– 62. doi: 10.1016/j.quascirev.2010.10.005.

Tan, L., Cai, Y., Cheng, H., An, Z., Edwards, R.L., 2009. Summer monsoon precipitation variations in central China over the past 750 years derived from a high-resolution absolute-dated stalagmite. Palaeogeogr. Palaeoclimatol. Palaeoecol. 280, 432– 439. doi: 10.1016/j.palaeo.2009.06.030.

Tierney, J.E., Oppo, D.W., Rosenthal, Y., Russell, J.M., Linsley, B.K., 2010. Coordinated hydrological regimes in the Indo-Pacific region during the past two millennia. Paleoceanography 25, PA1102. doi: 10.1029/2009PA001871.

Ummenhofer, C.C., D'Arrigo, R.D., Anchukaitis, K.J., Buckley, B.M., Cook, E.R., 2013. Links between Indo-Pacific climate variability and drought in the Monsoon Asia Drought Atlas. Clim. Dyn. 40, 1319– 1334. doi: 10.1007/s00382-012-1458-1.

Wang, B., Clemens, S.C., Liu, P., 2003. Contrasting the Indian and East Asian monsoons: Implications on geologic timescales. Mar. Geol. 201, 5–21. doi: 10.1016/S0025-3227(03)00196-8.

Wang, P., 2009. Global monsoon in a geological perspective. Chin. Sci. Bull. 54, 1113–1136. doi: 10.1007/s11434-009-0169-4.

Wang, P., Clemens, S., Beaufort, L., Braconnot, P., Ganssen, G., Jian, Z., Kershaw, P., Sarnthein, M., 2005a. Evolution and variability of the Asian monsoon system: State of the art and outstanding issues. Quat. Sci. Rev. 24, 595– 629. doi: 10.1016/j.quascirev.2004.10.002.

Wang, Y., Cheng, H., Edwards, R.L., He, Y., Kong, X., An, Z., Wu, J., Kelly, M.J., Dykoski, C.A., Li, X., 2005b. The holocene asian monsoon: links to solar changes and North Atlantic climate. Science 308, 854–857. doi: 10.1126/science.1106296.

Wannakomol, A., 2005. Soil and Groundwater Salinization Problems in the Khorat Plateau, NE Thailand Integrated Study of Remote Sensing, Geophysical and Field Data. Freie Universität Berlin, Berlin.

Wohlfarth, B., Klubseang, W., Inthongkaew, S., Fritz, S.C., Blaauw, M., Reimer, P.J., Chabangborn, A., Löwemark, L., Chawchai, S., 2012. Holocene environmental changes in northeast Thailand as reconstructed from a tropical wetland. Glob. Planet. Change 92– 93, 148– 161. doi: 10.1016/j.gloplacha.2012.05.008.

Yan, H., Sun, L., Oppo, D.W., Wang, Y., Liu, Z., Xie, Z., Liu, X., Cheng, W., 2011. South China Sea hydrological changes and Pacific Walker Circulation variations over the last millennium. Nat. Commun. 2, 293. doi: 10.1038/ncomms1297.

Yancheva, G., Nowaczyk, N.R., Mingram, J., Dulski, P., Schettler, G., Negendank, J.F.W., Liu, J., Sigman, D.M., Peterson, L.C., Haug, G.H., 2007. Influence of the intertropical convergence zone on the East Asian monsoon. Nature 445, 74– 77. doi: 10.1038/nature05431.

Zhang, P., Cheng, H., Edwards, R.L., Chen, F., Wang, Y., Yang, X., Liu, J., Tan, M., Wang, X., Liu, J., An, C., Dai, Z., Zhou, J., Zhang, D., Jia, J., Jin, L., Johnson, K.R., 2008. A test of climate, Sun, and culture relationships from an 1810-year Chinese cave record. Science 322, 940– 942. doi: 10.1126/science.1163965.